

Fast Hybrid Algorithms for High Frequency Scattering

Björn Engquist, Khoa Tran, and Lexing Ying

Citation: [AIP Conference Proceedings](#) **1106**, 3 (2009); doi: 10.1063/1.3117111

View online: <http://dx.doi.org/10.1063/1.3117111>

View Table of Contents:

<http://scitation.aip.org/content/aip/proceeding/aipcp/1106?ver=pdfcov>

Published by the [AIP Publishing](#)

Articles you may be interested in

[Scattering Properties of Chaotic Microwave Resonators](#)

[AIP Conf. Proc.](#) **1076**, 223 (2008); 10.1063/1.3046259

[An efficient high-order algorithm for acoustic scattering from penetrable thin structures in three dimensions](#)

[J. Acoust. Soc. Am.](#) **121**, 2503 (2007); 10.1121/1.2714919

[Computation of scattering from N spheres using multipole reexpansion](#)

[J. Acoust. Soc. Am.](#) **112**, 2688 (2002); 10.1121/1.1517253

[Time harmonic electromagnetic scattering from a bounded obstacle: An existence theorem and a computational method](#)

[J. Math. Phys.](#) **40**, 4859 (1999); 10.1063/1.533004

[An iterative solver of the Helmholtz integral equation for high-frequency acoustic scattering](#)

[J. Acoust. Soc. Am.](#) **103**, 742 (1998); 10.1121/1.421238

Fast Hybrid Algorithms for High Frequency Scattering

Björn Engquist*, Khoa Tran[†] and Lexing Ying**

*Department of Mathematics and ICES, University of Texas, Austin, TX 78712

[†]Institute of Computational Engineering and Sciences, University of Texas, Austin, TX 78712

**Department of Mathematics, University of Texas, Austin, TX 78712

Abstract. This paper deals with numerical methods for high frequency wave scattering. It introduces a new hybrid technique that couples a directional fast multipole method for a subsection of a scattering surface to an asymptotic formulation over the rest of the scattering domain. The directional fast multipole method is new and highly efficient for the solution of the boundary integral formulation of a general scattering problem but it requires at least a few unknowns per wavelength on the boundary. The asymptotic method that was introduced by Bruno and collaborators requires much fewer unknowns. On the other hand the scattered field must have a simple structure. Hybridization of these two methods retains their best properties for the solution of the full problem. Numerical examples are given for the solution of the Helmholtz equation in two space dimensions.

Keywords: High frequency scattering, Helmholtz equation, Boundary integral equation, Directional Fast multipole method, Hybrid method

PACS: 02.30.Rz, 02.60.Cb, 02.60.Nm, 02.70.Pt, 03.65.Nk

INTRODUCTION

In this paper, we consider the numerical solution of the time harmonic acoustic scattering problem. Suppose that $\Omega \subset \mathbb{R}^d$ ($d = 2, 3$) is a smooth impenetrable object with boundary $\Gamma = \partial\Omega$ and exterior normal $n(x)$ for $x \in \Gamma$. We assume that the wave number k is very large and the incoming wave is given by $u^I(x) = e^{ik\alpha \cdot x}$ with $|\alpha| = 1$. The scattered wave field $u(x)$ then satisfies the following Helmholtz equation with Dirichlet boundary condition

$$\begin{aligned} \Delta u(x) + k^2 u(x) &= 0 \quad \text{for } x \in \mathbb{R}^2 \setminus \bar{\Omega} \\ u(x) &= -u^I(x) \quad \text{for } x \in \Gamma \\ \lim_{|x| \rightarrow \infty} |x|^{(d-1)/2} \left(\left(\frac{x}{|x|}, \nabla u(x) \right) - ik u(x) \right) &= 0, \end{aligned} \tag{1}$$

where the last condition is the *Sommerfeld radiation condition* and guarantees that the scattered field $u(x)$ propagates to infinity.

The numerical solution of this problem often starts by transforming it into a boundary integral equation with an unknown density supported on Γ . The main advantage is that now one works with a lower dimensional problem on a bounded domain. One possible

approach [1, 2] is to write the scattered field $u(x)$ as a single layer potential:

$$u(x) = - \int_{\Gamma} G(x,y)\mu(y)ds(y) \quad \text{with} \quad G(x,y) = \begin{cases} \frac{i}{4}H_0^{(1)}(k|x-y|) & (d=2) \\ \frac{1}{4\pi} \frac{e^{ik|x-y|}}{|x-y|} & (d=3) \end{cases} \quad (2)$$

where $G(x,y)$ is the Green's function of the Helmholtz operator and $\mu(x) = \frac{\partial(u(x)+u^l(x))}{\partial n(x)}$ for $x \in \Gamma$ is the normal derivative of the total field. It can be shown that the boundary density $\mu(x)$ is the unique solution of the following combined field integral equation

$$\frac{1}{2}\mu(x) + \int_{\Gamma} \left(\frac{\partial G(x,y)}{\partial n(x)} - i\gamma G(x,y) \right) \mu(y)ds(y) = \frac{\partial u^l(x)}{\partial n(x)} - i\gamma u^l(x) \quad (3)$$

with $\gamma > 0$. To simplify the notation, we will denote the combined kernel $\left(\frac{\partial G(x,y)}{\partial n(x)} - i\gamma G(x,y) \right)$ by $K(x,y)$. By choosing $\gamma \approx k$, this equation has a condition number that is almost independent of k (see [3]). For high frequency scattering problems, k is typically very large and therefore the density $\mu(x)$ is often highly oscillatory.

In the past twenty years, there has been a substantial amount of research devoted to the rapid solution of (3). Since $\mu(x)$ is often discretized numerically with a constant number of unknowns per wavelength $\lambda = 2\pi/k$, the number of unknowns scales like $O(k^{d-1})$ and the discrete version of (3) has a dense $O(k^{d-1}) \times O(k^{d-1})$ matrix. As a result, iterative methods such as GMRES are the natural tools for the solution of (3). At each step of the iterative solver, one needs to perform a matrix vector product that simply takes $O(k^{2(d-1)})$ operations in a naive implementation. One active line of research aims to compute this matrix vector product in $O(k \log k)$ steps. Two examples are the high frequency fast multipole method (HF-FMM) developed by Rokhlin et al. [4, 5, 6, 7, 8] and the recently proposed directional fast multipole method [9, 10] by two of the authors of this article. Combined with an accurate quadrature rule, these methods can offer accurate and efficient algorithms for solving (3) with almost linear complexity in the number of unknowns.

Another line of research leverages the asymptotic results from geometrical optics [11] for convex scatterers and has recently experienced a lot of exciting developments [12, 1, 13, 14, 15]. The main observation there is that when the scatterer is smooth and convex, the density $\mu(x)$ can be decomposed as the product of a slowly varying amplitude and an oscillatory term with the same phase as the incoming wave. As a result, one only needs to solve for the amplitude function. In fact, for a fixed tolerance, the amplitude can be approximated with a small set of basis functions with a cardinality independent of k . The computation of the discrete linear operator can also be done in $O(1)$ operations with the help of novel integration schemes such as the localized integrators [1] or the oscillatory quadrature rules [15]. However, such an approach works mostly for convex scatterers, as for non-convex objects multiple reflections break the simple decomposition of $\mu(x)$. Some recent developments on simple multiple scattering cases are discussed in [16, 2].

In this paper, we focus on the two dimensional case where the scatterer can be represented as a combination of a large convex object and a small structure (see Figure 1 for an example). A practical application can be an antenna on a large object as, for

example a building or an airplane. For simplicity, we assume that the small structure is of size $O(k^{-1/2})$. For scatterers of this type, neither of the two aforementioned methods are optimal. Here, we propose a hybrid integral equation method that combines the advantages of these two approaches and has an $O(k^{1/2} \log k)$ complexity. On the one hand, we discretize the small structure densely with a constant number of samples per wavelength and use the directional fast multipole method to speed up the computation. On the other hand, the geometrical optics based approach discretizes the large body sparsely. A smooth partition of unity merges these two representations together seamlessly.

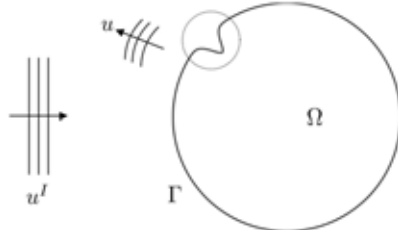


FIGURE 1. The scattering of an incoming plane wave u^l from a smooth scatterer Ω . u is the scattered field. The boundary Γ of the scatterer can be represented as a large convex part and a small structure (inside the small circle).

The rest of this paper is organized as follows. First, we briefly review the directional fast multipole method proposed in [9, 10] and also introduce some improvements. Then we outline the geometrical optics based method, mostly following the presentation of [1]. Next, we present the hybrid method, together with preliminary numerical results. Finally, we conclude with a discussion of future directions.

THE DIRECTIONAL FAST MULTIPOLE METHOD

In this section, we briefly discuss the directional fast multipole method proposed in [9, 10] in the two dimensional form. Let us assume that the integral equation (3) is solved with a Nyström method. With a few unknowns per wavelength, the integral in (3) is discretized with a set of $N = O(k)$ equally spaced quadrature points $\{x_i\}_{1 \leq i \leq N}$ on Γ . Let $\{\mu_i\}$ to be the approximations to $\{\mu(x_i)\}$. Then the discretized system takes the following form:

$$\frac{1}{2}\mu_i + \sum_{j=1}^N K(x_i, x_j)w_{ij} \cdot \mu_j = \frac{\partial u^l(x_i)}{\partial n(x_i)} - i\gamma u^l(x_i) \quad (4)$$

where w_{ij} are the quadrature weights. Often we choose w_{ij} so that, for a fixed i , the weights w_{ij} become i independent when $|i - j| \geq C$ for a constant C independent of k . As we mentioned earlier, this system is often solved with an iterative method such as GMRES and the main computational task within each iteration is then to evaluate the

potentials

$$u_i = \sum_{j=1}^N G(x_i, x_j) f_j, \quad 1 \leq i \leq N \quad (5)$$

for a given set of sources $\{f_j\}_{1 \leq j \leq N}$. Here, we consider only the kernel $G(x, y)$, and the treatment for $\frac{\partial G(x, y)}{\partial n(x)}$ is similar.

The directional fast multipole method proposed in [9, 10] evaluates all $\{u_i\}_{1 \leq i \leq N}$ in $O(N \log N) = O(k \log k)$ steps. It starts by building an adaptive quadtree for the whole scatterer (see Figure 2(a)). The whole domain is partitioned dyadically and recursively until that all of the leaf squares have side length equal to $\lambda = 2\pi/k$. Since the boundary Γ is smooth and only a constant number of points is used per wavelength, each leaf square contains only a small number of quadrature points x_i . For a square B with side length $w\lambda$, we define its *far field* F^B to be the region that is $O(w^2\lambda)$ away from B . The complement of F^B is called B 's *near field* and is denoted by N^B . A square A of the same side length is said to be in the *interaction list* of B if A is in B 's far field but not B 's parent's far field. The far field F^B is further partitioned into a group of $O(w)$ directional wedges $\{W^{B, \ell}\}$, each contained in a cone with center direction ℓ and spanning angle $O(1/w)$ (see Figure 2(b)).

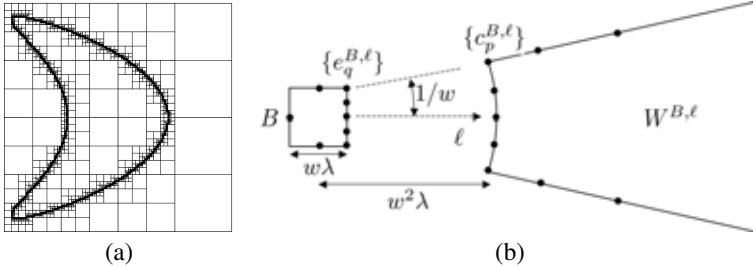


FIGURE 2. (a) The quadtree of a kite-shaped scatterer. (b) The square B and one of its wedges $W^{B, \ell}$. The points $\{e_q^{B, \ell}\}_{1 \leq q \leq r_\varepsilon}$ and $\{c_p^{B, \ell}\}_{1 \leq p \leq r_\varepsilon}$ are used in the separated approximation (6).

The main idea behind the directional fast multipole method is a directional low rank property of the Helmholtz kernel between B and each wedge $W^{B, \ell}$. It can be shown that, for any prescribed accuracy ε , there exists a rank- r_ε separated approximation of $G(x, x')$ for $x' \in B$ and $x \in W^{B, \ell}$:

$$\left| G(x, x') - \sum_{q=1}^{r_\varepsilon} G(x, e_q^{B, \ell}) \sum_{p=1}^{r_\varepsilon} d_{qp}^{B, \ell} G(c_p^{B, \ell}, x') \right| \leq \varepsilon, \quad (6)$$

with $\{e_q^{B, \ell}\}_{1 \leq q \leq r_\varepsilon} \subset B$, $\{c_p^{B, \ell}\}_{1 \leq p \leq r_\varepsilon} \subset W^{B, \ell}$. The points $\{e_q^{B, \ell}\}_{1 \leq q \leq r_\varepsilon}$, $\{c_p^{B, \ell}\}_{1 \leq p \leq r_\varepsilon}$, and the matrix $D^{B, \ell} = (d_{qp}^{B, \ell})_{1 \leq p, q \leq r_\varepsilon}$ can be computed efficiently by a randomized procedure proposed in [10]. It is important to point out that the rank r_ε is independent of w , i.e., the ratio between the size of B and the wavelength λ .

The separated approximation (6) allows us to construct a compact representation for the potential in $W^{B, \ell}$ generated by the points in B . After applying the separated

approximation in (6) to $x' = x_i \in B$ and summing them up with weights f_i , we obtain

$$\left| \sum_{x_i \in B} G(x, x_i) f_i - \sum_{q=1}^{r_\varepsilon} G(x, e_q^{B, \ell}) \left(\sum_{p=1}^{r_\varepsilon} d_{qp}^{B, \ell} \left(\sum_{x_i \in B} G(c_p^{B, \ell}, x_i) f_i \right) \right) \right| \leq \left(\sum_{x_i \in B} |f_i| \right) \varepsilon.$$

This implies that by placing a set of sources $\left\{ f_q^{B, \ell} = \sum_p d_{qp}^{B, \ell} \left(\sum_{x_i \in B} G(c_p^{B, \ell}, x_i) f_i \right) \right\}_{1 \leq q \leq r_\varepsilon}$ at points $\{e_q^{B, \ell}\}_{1 \leq q \leq r_\varepsilon}$ we can approximate at any $x \in W^{B, \ell}$ the potential generated by the sources in B . We call $\left\{ f_q^{B, \ell} \right\}_{1 \leq q \leq r_\varepsilon}$ the *directional outgoing equivalent sources of B in direction ℓ* . In our setting, they play the role of the multipole expansions in the FMM algorithm [17, 18]. It is clear from the definition that the computation of $\{f_q^{B, \ell}\}_{1 \leq q \leq r_\varepsilon}$ uses only kernel evaluations and a matrix vector product with the $r_\varepsilon \times r_\varepsilon$ matrix $D^{B, \ell}$.

Similarly, the approximation (6) also provides us with a compact representation for the potential in B generated by the points in $W^{B, \ell}$. Since $G(x, y) = G(y, x)$, summing over $x_i \in W^{B, \ell}$ with weights f_i leads us to

$$\left| \sum_{x_i \in W^{B, \ell}} G(x', x_i) f_i - \sum_{p=1}^{r_\varepsilon} G(x', c_p^{B, \ell}) \left(\sum_{q=1}^{r_\varepsilon} d_{qp}^{B, \ell} \left(\sum_{x_i \in W^{B, \ell}} G(e_q^{B, \ell}, x_i) f_i \right) \right) \right| \leq \left(\sum_{x_i \in W^{B, \ell}} |f_i| \right) \varepsilon.$$

This means that, from the potentials $\{u_q^{B, \ell} = \sum_{x_i \in W^{B, \ell}} G(e_q^{B, \ell}, x_i) f_i\}_{1 \leq q \leq r_\varepsilon}$ at points $\{e_q^{B, \ell}\}_{1 \leq q \leq r_\varepsilon}$, we can compute at any $x' \in B$ the potential generated by $x_i \in W^{B, \ell}$ through a matrix vector product with $D^{B, \ell}$ and kernel evaluations. These potentials $\{u_q^{B, \ell}\}_{1 \leq q \leq r_\varepsilon}$ are called the *directional incoming check potentials of B in direction ℓ* . In our algorithm, they play the role of the local expansions of the FMM algorithm.

Another important component of our algorithm is the translation operators that transform the compact representations introduced above. Following the convention in [4, 18], we call them the M2M, L2L, and L2L translations. Since by definition the wedges of the parent square and the child square are nested, for each square B and one of its directions ℓ , we can find a direction ℓ' such that $W^{B, \ell} \subset W^{B_c, \ell'}$ for every child B_c of B . The M2M translation then constructs the outgoing directional equivalent sources of $\{f_q^{B, \ell}\}_{1 \leq q \leq r_\varepsilon}$ of B in direction ℓ from the outgoing equivalent sources of B 's children in direction ℓ' . More precisely, it takes $\{f_{q'}^{B_c, \ell'}\}_{c, q'}$ located at $\{e_{q'}^{B_c, \ell'}\}_{c, q'}$ as the true sources and performs the following computation:

$$f_q^{B, \ell} \Leftarrow \sum_p d_{qp}^{B, \ell} \left(\sum_c \sum_{q'} G(c_p^{B, \ell}, e_{q'}^{B_c, \ell'}) f_{q'}^{B_c, \ell'} \right). \quad (7)$$

On the other hand, the L2L translation constructs the incoming directional check potentials of B 's children at direction ℓ' from the the incoming directional check potentials $\{u_q^{B, \ell}\}_{1 \leq q \leq r_\varepsilon}$ of B at directional ℓ :

$$u_{q'}^{B_c, \ell'} \Leftarrow u_{q'}^{B_c, \ell'} + \sum_p G(e_{q'}^{B_c, \ell'}, c_p^{B, \ell}) \left(\sum_q d_{qp}^{B, \ell} u_q^{B, \ell} \right). \quad (8)$$

Finally, the M2L translation is applied to all pairs of squares A and B that are in each other's interaction list. Suppose that B is in the wedge $W^{A,\ell}$ of A and that A is in the wedge $W^{B,\ell}$ of B . The M2L translation uses $\{f_{q'}^{A,\ell}\}_{1 \leq q' \leq r_\epsilon}$ to update $\{u_q^{B,\ell}\}_{1 \leq q \leq r_\epsilon}$:

$$u_q^{B,\ell} \Leftarrow u_q^{B,\ell} + \sum_{q'} G(e_q^{B,\ell}, e_{q'}^{A,\ell}) f_{q'}^{A,\ell}. \quad (9)$$

Putting these components together leads us to the following *directional fast multipole method*.

1. Construct the quadtree adaptively. The whole domain is partitioned dyadically and recursively until that all of the leaf squares have side length equal to λ . Then each leaf square contains a small number of points.
2. Travel up the quadtree. For each square B and each direction ℓ , if B is a leaf, construct $\{f_q^{B,\ell}\}_{1 \leq q \leq r_\epsilon}$ using

$$f_q^{B,\ell} \Leftarrow \sum_p a_{qp}^{B,\ell} \sum_{x_i \in B} G(c_p^{B,\ell}, x_i) f_i.$$

If B is not a leaf, construct $\{f_q^{B,\ell}\}_{1 \leq q \leq r_\epsilon}$ using the M2M translation (7).

3. Travel down the quadtree. For each square B and each direction ℓ , perform the following two steps:
 - (a) For each A in B 's interaction list and in $W^{B,\ell}$ update $\{u_q^{B,\ell}\}_{1 \leq q \leq r_\epsilon}$ using the M2L translation.
 - (b) If B is not a leaf, perform the L2L translation (8) to transform $\{u_q^{B,\ell}\}$ to the incoming check potentials for B 's children. If B is a leaf, perform for $x_i \in B$

$$u_i \Leftarrow u_i + \sum_p G(x_i, c_p^{B,\ell}) \left(\sum_q d_{qp}^{B,\ell} u_q^{B,\ell} \right).$$

4. Nearby interaction. For each leaf square B , for each $x_i \in B$, perform

$$u_i \Leftarrow u_i + \sum_{x_j \in N^B} G(x_i, x_j) f_j.$$

It can be shown that, for the quadrature points $\{x_i\}$ distributed uniformly on Γ , this algorithm takes at most $O(k \log k)$ steps (see [9] for the proof). As we mentioned earlier, for a fixed scatterer, the iterative solution of (4) often converges after a constant number of iterations that is independent of k . Therefore, the total number of steps for solving (4) is also $O(k \log k)$.

THE GEOMETRICAL OPTICS BASED APPROACH

Before we present the geometrical optics (GO) based boundary integral method let us discuss a few relevant aspects of general high frequency asymptotics.

Classical geometrical optics

The simplest form of high frequency asymptotics for the Helmholtz equation (1) is based on the assumption that the solution has the following form as $k \rightarrow \infty$,

$$u(x) = e^{ik\phi(x)}A(x, k) = e^{ik\phi(x)} \sum_{j=0}^{\infty} A_j(x)k^{-j}, \quad (10)$$

where $\phi(x)$ is the phase and $A(x)$ the amplitude. When the Helmholtz operator is applied to this expression we can derive the eikonal equation for the phase, ($c(x)$ is the wave speed)

$$|\nabla\phi(x)| = 1/c(x) \quad (11)$$

and the transport equations for the amplitudes $A_j(x)$. The most common formulation of GO is via the ray equations, which define the bicharacteristics of the eikonal equation,

$$\begin{aligned} \frac{dx}{dt} &= \frac{c(x)p}{|p|} \\ \frac{dp}{dt} &= -|p|\nabla c(x). \end{aligned}$$

As long as the solution has this simple form of a well defined phase and amplitude the error in the geometrical optics approximation based on the leading term in the expansion (11) is of order $O(1/k)$.

When boundaries are present the simple form above is not valid any longer. Reflections determined by Snell's law add other phases such that the solution becomes a superposition of components of the form (10),

$$u(x) = \sum_{n=1}^N e^{ik\phi_n(x)}A^{(n)}(x, k). \quad (12)$$

Geometrical theory of diffraction (GTD) is an improvement of GO that includes diffraction terms in the expansion (12) for higher accuracy. Another form of high frequency approximation is physical optics (PO), which is based on an integral representation of type (2). The approximation in PO comes from the simple algorithm for computing $\mu(x)$,

$$\mu(x) = \begin{cases} 2\frac{\partial u^I(x)}{\partial n(x)} & x \text{ in the illuminated region} \\ 0 & x \text{ in the shadow region} \end{cases}$$

These asymptotic formulas can sometimes be verified by rigorous mathematics and one such case is the scattering of a harmonic plane wave off a convex object [19]. The scattered field and the density $\mu(x)$ has essentially the form (10) where $\phi(x)$ is given by the incident phase. This is the mathematical foundation of the GO based boundary integral method.

The GO based integral equation method

Motivated by the classical GO method, recently there has been a lot of activities [12, 1, 13, 14, 15] in combining the asymptotic results with the integral equation formulation. Here, our description follows the Nyström method proposed in [1]. The main observation is that when the scatterer Ω is convex the density $\mu(x)$ can be decomposed as a product of a slowly varying amplitude $\mu^s(x)$ and an oscillatory term with the phase of the incoming wave, i.e.,

$$\mu(x) = \mu^s(x)e^{ik\alpha \cdot x}. \quad (13)$$

Substituting this decomposition into (3) gives the following integral equation of the slow density $\mu^s(x)$

$$\frac{1}{2}\mu^s(x) + \int_{\Gamma} K(x,y)e^{ik\alpha \cdot (y-x)}\mu^s(y)ds(y) = ik\alpha \cdot n(x) - i\gamma. \quad (14)$$

In the rest of this paper, we denote the new kernel $K(x,y)e^{ik\alpha \cdot (y-x)}$ by $K^s(x,y)$.

Since the scatterer Ω is convex, for a fixed incoming plane wave there are exactly two shadow points on the boundary. To describe the qualitative behavior of the slow density $\mu^s(x)$, one decomposes the boundary into four disjoint parts [19]: the illuminated region facing the incoming wave, the shadow region, and two boundary regions. Each of the boundary region is centered around one shadow point and is of size $O(k^{-1/3})$ (see Figure 3(a)).

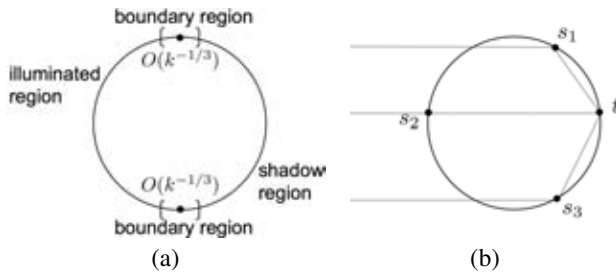


FIGURE 3. (a) The smooth convex scatterer is decomposed into four parts: illuminated region, shadow region, and two boundary regions. (b) For a target point t , the localized integrator is applied at the three stationary points s_1 , s_2 , and s_3 .

In both the illuminated and shadow regions, $\mu^s(x)$ varies on the scale of $O(1)$. Therefore, in order to approximate $\mu^s(x)$ in the illuminated and shadow regions, one only needs to sample $\mu^s(x)$ in these two regions with a constant number of Nyström points. In each boundary region, $\mu^s(x)$ is more oscillatory and varies on the scale $O(k^{-1/3})$. However, since each boundary region is of size $O(k^{-1/3})$, we only need a constant number of Nyström points to approximate the density $\mu^s(x)$ in these two boundary regions as well. Therefore, the total number of Nyström points required to represent $\mu^s(x)$ is independent of k for a prescribed accuracy. In [1], this is done by introducing a smooth boundary parameterization with derivative of order $O(k^{-1/3})$ in the boundary regions and of order $O(1)$ away from them. The boundary Γ is then sampled uniformly according to this new parameterization with a constant number of Nyström points $\{x_i\}$.

The second component of the Nyström method is the approximation of the integral

$$\int_{\Gamma} K^s(x, y) \mu^s(y) ds(y) = \int_{\Gamma} \left(\frac{\partial G(x, y)}{\partial n(x)} - i\gamma G(x, y) \right) e^{ik\alpha(y-x)} \mu^s(y) ds(y) \quad (15)$$

for each $x = x_i$, with $\mu^s(y)$ represented by its values at the Nyström points $\{x_i\}$. Given a fixed x , the asymptotic expansion of the Hankel functions shows that the phase of the kernel $K^s(x, y)$ for large values of k is given by

$$e^{ik(|x-y| + \alpha \cdot (y-x))}$$

when $y \neq x$. Since $\mu^s(y)$ varies much slower, a stationary phase argument shows that the main contribution of the integral (15) (away from $y = x$) comes from the neighborhoods of the stationary points, i.e., the points y that satisfy

$$\frac{d}{ds(y)} (|x-y| + \alpha \cdot (y-x)) = 0.$$

Therefore, in order to integrate (15) up to a fixed accuracy, it is sufficient to consider only two types of contributions: (1) the integral localized near the target point x when the kernel $K^s(x, y)$ is singular and (2) the integrals localized near the stationary points. In [1], this localization is done efficiently by using smooth window functions of appropriate size:

- A smooth window function of width $O(k^{-1})$ localizes the integral near the target point x . Since the kernel oscillates on the scale $O(k^{-1})$ near the target point x , a constant number of sample points near x are sufficient to approximate it up to a fixed accuracy.
- A smooth window function of width $O(k^{-1/2})$ localizes the integral near each stationary point. Since the kernel oscillates on the scale $O(k^{-1/2})$ near the stationary point, again only a constant number of samples are required.

Therefore, in order to integrate (14) for each $x = x_i$, we only need to sample at a constant number of points in total.

The situation is slightly more complicated when the target point $x = x_i$ is at (or close to) the boundary point. In this case, the kernel $K^s(x, y)$ as a function of y oscillates on the scale $O(k^{-1})$ on one side of the target point, while on the other side it has the phase of a stationary point of order 2 (see Figure 4). In order to integrate this asymmetric behavior, one solution is to place a half window function on each side of x . The window function on the highly oscillatory side is of width $O(k^{-1})$, while the one on the opposite side is of width $O(k^{-1/3})$. Within each window function, we use a generalized Gaussian quadrature rule with a constant of points to approximate the integral.

In the above discussion, we make the assumption that one can sample the density $\mu^s(x)$ freely at any point on the boundary. However, in the Nyström method, the density $\mu^s(x)$ is only provided at the Nyström points $\{x_i\}$ and, thus, we need a method to interpolate $\mu^s(x)$ at arbitrary points on Γ from its values at $\{x_i\}$. The natural solution for smooth scatterers is the nonuniform fast Fourier transform [20, 21], which allows us to sample at M arbitrary points in $O(M \log M)$ operations.

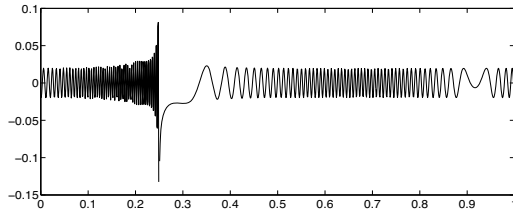


FIGURE 4. The behavior of the kernel $K^s(x, y)$ as a function of y when x is at the shadow point.

The GO based boundary integral equation method is often mentioned as a technique that for a given geometry of a simple form, incident harmonic plane wave and given error tolerance can generate a solution with a computational complexity that is independent of the wave number k . With respect to k this would mean an $O(1)$ complexity strategy. This is not spectacular in itself since a simple combination of standard GO and MM also achieves this goal. With given geometry, incoming field and error tolerance we can choose a cut off frequency such that geometrical optics is accurate enough above this frequency and then choose any boundary integral method for problems below this frequency. Recall the $O(1/k)$ error estimate above. The GO based boundary integral method is however much more seamless and has the potential of higher efficiency.

If there are more phases involved in the solution (12) the boundary integral methods require a GO pre-processing step in order to determine the phases in the boundary potential [2]. This is why we are including GO in the name of the name of the method. In our conclusions we suggest an alternative, which would make the technique even more seamless.

THE HYBRID METHOD

In many applications that involve high frequency scattering, the scatterers can often be represented as a combination of a large convex part and a complicated small structure (see Figure 5(a)). One typical example is an antenna on a building. For an scatterer of this type, the ansatz in (13) is often only valid for the large convex part, while the density $\mu(x)$ can be arbitrarily oscillatory at the small structure. As a result, neither method discussed in the previous two sections is optimal when k is very large and the small structure is, for example, of size $O(k^{-1/2})$. The method based on the directional fast multipole method samples the whole boundary densely even though the density $\mu(x)$ has an efficient representation for the most part of the boundary; on the other hand the GO based integral equation method faces difficulty in handling the non-convex part. In this section, we discuss a hybrid method that combines the advantages of both methods. The main idea is simply to partition the boundary into two overlapping parts and then use the appropriate representation for each part.

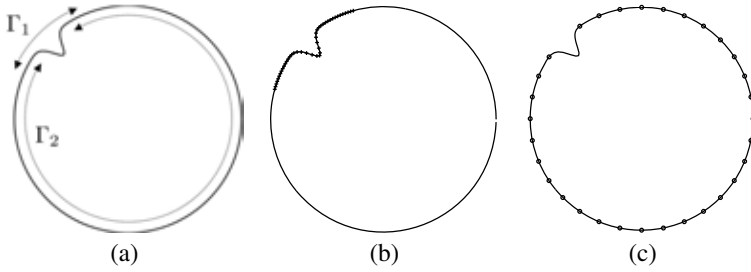


FIGURE 5. (a) The boundary of the scatterer is represented as the union of Γ_1 and Γ_2 . Γ_1 contains the small structure while Γ_2 covers the large convex part. (b) The sample points P_1 in the dense discretization of Γ_1 . (c) The sample points P_2 in the sparse discretization of Γ_2 .

Algorithm description

We start by introducing an open covering $\{\Gamma_1, \Gamma_2\}$ of the boundary Γ (see Figure 5(a)). Γ_1 covers the small structure and is of size $O(k^{-1/2})$, Γ_2 contains only the large convex part, and the size of the overlapping region $\Gamma_1 \cap \Gamma_2$ is of order $O(k^{-1/2})$. Next, we construct a partition of unity $\{\alpha_1(x), \alpha_2(x)\}$ subordinate to the covering $\{\Gamma_1, \Gamma_2\}$, i.e.,

$$\alpha_1(x) + \alpha_2(x) = 1, \quad \text{supp}(\alpha_1) \subset \Gamma_1, \quad \text{supp}(\alpha_2) \subset \Gamma_2.$$

Since $\Gamma_1 \cap \Gamma_2$ is of size $O(k^{-1/2})$, we can make $\alpha_1(x)$ and $\alpha_2(x)$ to vary on a scale of $O(k^{-1/2})$.

Similar to the two methods described in the previous two sections, we adopt a Nyström discretization for the solution of (3). Let us estimate how many samples are required in order to approximate $\mu(x)$ to a fixed accuracy. We first consider the restriction of $\mu(x)$ to Γ_1 . The oscillation of $\mu(x)$ on Γ_1 can be quite arbitrary, depending on the shape of the small structure. However, since Γ_1 is of size $O(k^{-1/2})$, we only need to sample $\mu(x)$ at a set of $O(k^{-1/2}/k^{-1}) = O(k^{1/2})$ equally spaced samples P_1 in Γ_1 (see Figure 5(b)). Second, $\mu(x)$ on Γ_2 has a simple form $\mu(x) = \mu^s(x)e^{ik\alpha \cdot x}$. Therefore, in order to approximate $\mu(x)$ on Γ_2 , we sample $\mu(x)$ on Γ_2 with a small number of samples P_2 at a rate much lower compared to the Nyquist rate, compute $\mu^s(x)$ for $x \in P_2$ by multiplying $e^{-ik\alpha \cdot x}$, interpolate $\mu^s(x)$ for $x \in \Gamma_2$ from its values at P_2 , and finally multiply by $e^{ik\alpha \cdot x}$ to obtain the approximation of $\mu(x)$ on Γ_2 . In practice, we set P_2 to be a set of $O(k^{1/2})$ equally spaced samples with spacing $O(k^{-1/2})$ (see Figure 5(c)). By putting P_1 and P_2 together, we see that one only needs $O(k^{1/2})$ Nyström points to represent $\mu(x)$.

The second component of our Nyström method is the evaluation of the integral

$$\int_{\Gamma} K(x, y) \mu(y) ds(y) = \int_{\Gamma} \left(\frac{\partial G(x, y)}{\partial n(x)} - i\gamma G(x, y) \right) \mu(y) ds(y) \quad (16)$$

given the values of $\mu(x)$ at $x_i \in P_1 \cup P_2$. Based on the partition of unity $\{\alpha_1(x), \alpha_2(x)\}$, we can represent $\mu(x)$ as a sum of two parts:

$$\mu(x) = \alpha_1(x)\mu(x) + \alpha_2(x)\mu(x).$$

Using this decomposition to rewrite the integral (16) gives

$$\begin{aligned} \int_{\Gamma} K(x,y)\mu(y)ds(y) &= \int_{\Gamma} K(x,y)\alpha_1(y)\mu(y)ds(y) + \int_{\Gamma} K(x,y)\alpha_2(y)\mu(y)ds(y) \\ &= \int_{\Gamma_1} K(x,y)\alpha_1(y)\mu(y)ds(y) + \int_{\Gamma_2} K(x,y)\alpha_2(y)\mu(y)ds(y) \end{aligned} \quad (17)$$

where in the last step we use the facts that support of $\alpha_t(y)$ is Γ_t for $t = 1, 2$.

To calculate the first integral, we discretize it using the quadrature points $x_j \in P_1$, i.e.,

$$\sum_{x_j \in \Gamma_1} K(x, x_j) w_{ij} \cdot \alpha_1(x_j) \mu(x_j)$$

where w_{ij} are the quadrature weights in (4). Evaluating the above quantities for all $x_i \in P_1 \cup P_2$ is exactly the problem addressed earlier, yet on a much smaller scale, since the number of points in $P_1 \cup P_2$ is only of order $O(k^{1/2})$ now. Therefore, by using the directional fast multipole method, we can evaluate the first integral for *all* $x = x_i \in P_1 \cup P_2$ with at most $O(k^{1/2} \log k)$ operations.

To address the second integral, we substitute the ansatz $\mu(y) = \mu^s(y)e^{ik\alpha \cdot y}$ for $y \in \Gamma_2$:

$$e^{ik\alpha \cdot x} \cdot \int_{\Gamma_2} K(x,y)e^{ik\alpha \cdot (y-x)} \alpha_2(y) \mu^s(y) ds(y) = e^{ik\alpha \cdot x} \cdot \int_{\Gamma_2} K^s(x,y) \cdot \alpha_2(y) \mu^s(y) ds(y).$$

Since $\alpha_2(y)\mu^s(y)$ is a slowly oscillating function, we can resort to the localized integration discussed in the previous section. As a result, for each point $x = x_i \in P_1 \cup P_2$, we only need to sample at $O(1)$ locations. Since there are at most $O(k^{1/2})$ quadrature points in $P_1 \cup P_2$, it takes at most $O(k^{1/2})$ steps to the evaluating the second integral for all quadrature points $x_i \in P_1 \cup P_2$.

To summarize, it takes at most $O(k^{1/2} \log k)$ steps to evaluate (16) for all quadrature points in $P_1 \cup P_2$. As we pointed out earlier, for a fixed scatterer, the iterative solution of (3) often converges after a constant number iterations. Therefore, the hybrid approach has a total time complexity bounded by $O(k^{1/2} \log k)$ as well.

We would like to point out that the classical geometrical optics methods applied to a sub domain of the scattering object have been hybridized in the literature with full numerical boundary integral techniques applied to the remaining part of the scattered. The name method of moments (MM) or (MoM) is often used instead of numerical boundary integral methods. Examples of the coupling GTD-MM and of PO-MM are given in [22, 23]. The new aspects of the hybrid method in this paper are that two very recent and highly efficient methods are involved and also that the technique naturally allows for a full two way coupling.

Numerical illustration

In this section, we present some preliminary numerical results for the hybrid method described above. Our test example is the object displayed in Figure 5 and its boundary is parameterized by

$$x = (r(\theta) \cos \theta, r(\theta) \sin \theta), \quad \text{with} \quad r(\theta) = 1 - \frac{8}{k} e^{-k(\pi - (\theta + 0.9) \bmod (2\pi))^2} \quad (18)$$

for $\theta \in [0, 2\pi)$. Here, we set $k = 100$.

Figure 6 shows the true solution $\mu^s(x)$, computed using a direct solver with dense discretization and Figure 7 shows the absolute value of the difference between the true solution and the approximated solution computed using the hybrid method. In this example, we use $6\sqrt{k}$ Nyström points both for the dense and sparse regions (Γ_1 and Γ_2). The integration in the dense region is computed by using the trapezoidal quadrature rule and the integration in the sparse region is computed by the localized integration technique with 150 discretization points for each localized integrator. Our GMRES solver for this hybrid method converges after 13 iterations to an approximated solution with an L_2 error of 0.003.

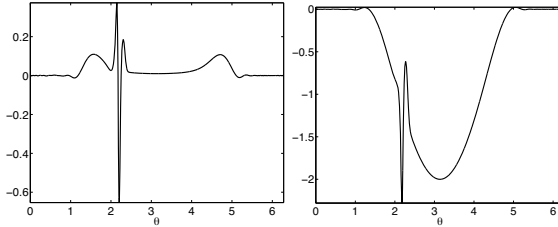


FIGURE 6. The real and imaginary parts of $\mu^s(x)$. The scatterer is given by the formula in (18) and $k = 100$. $\mu^s(x)$ is smooth in the convex part and is highly oscillatory in the small non-convex structure.

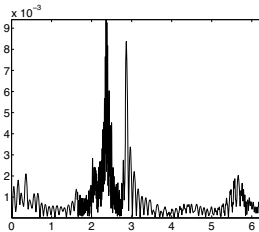


FIGURE 7. The absolute value of the difference between the true solution and the solution computed using the hybrid method.

If the small structure is of a size smaller than $O(k^{-1/2})$, the partition of unity function $\alpha_2(x)$ will be too sharp in the region Γ_2 . Hence, we cannot use a sparse representation for $\alpha_2(x)\mu^s(x)$ in this region. To overcome this problem, one can use a change of variable to stretch $\alpha_2(x)$ so that we can represent $\alpha_2(x)\mu^s(x)$ by a constant number of Nyström points.

We can further speed up the computation of the second integral of (17) significantly when the small structure in Γ_1 is relatively smooth. In the current form, our hybrid method performs the localized integration for each Nyström point $x_i \in P_1$. Instead, we can perform the localized integrator at few points in Γ_1 and then use Fourier or spline interpolation to obtain the values at the Nyström points $x_i \in P_1$.

CONCLUSIONS

Two efficient existing numerical techniques for high frequency wave scattering and their hybridization have been presented. The directional fast multipole method can handle general geometries and general scattered fields but require a positive number of unknowns per wavelength. The geometrical optics based boundary integral method by Bruno and collaborators requires much fewer unknowns but only applies to simpler geometries and scattered fields.

Our analysis and simple two-dimensional numerical model problem show the potential for hybridization of the two methods into a technique that exploits the best properties of both methods. The low computational complexity of the geometrical optics based method can essentially be retained even if the geometry locally requires a fine discretization.

A natural next step is to allow for more than one phase in the geometrical optics based technique in order to incorporate a full two-way interaction in the hybridization. Another extension will be to problems in three dimensions. The directional fast multipole method already exists as general three-dimensional software, [1] and the geometrically based technique have been applied to simple but nontrivial geometries also in three dimensions, [24, 25].

One problem with the geometrical optics based boundary integral method is the necessary ray tracing pre processing. If we do not have the simple case of a plane wave field scattered by a convex body, we must first solve the geometrical optics problem for the phases of all relevant waves in the asymptotic form. It is possible to integrate the detection of the relevant phases into the algorithm by finding the phases directly from the integral formulation. The field at any point in space can be calculated from the surface potential. This field can then be decomposed into a finite number of plane wave fields, see [26]. The implementation of such a process would generate a more seamless algorithm and be of value in itself and, in particular, in a hybridization of the form discussed in this paper.

ACKNOWLEDGMENTS

We would like to thank Olof Runborg and Christophe Geuzaine for insightful discussions. Engquist is partially supported by an NSF grant DMS 0714612 and a startup grant from the University of Texas at Austin. Ying is partially supported by an Alfred P. Sloan Research Fellowship and a startup grant from the University of Texas at Austin.

REFERENCES

1. O. P. Bruno, C. A. Geuzaine, J. A. Monro, Jr., and F. Reitich, *Philos. Trans. R. Soc. Lond. Ser. A Math. Phys. Eng. Sci.* **362**, 629–645 (2004), ISSN 1364-503X.
2. F. Ecevit, and F. Reitich, Analysis of multiple scattering iterations for high-frequency scattering problems. i: The two-dimensional case, Tech. rep., Preprint (2006).
3. D. Colton, and R. Kress, *Inverse acoustic and electromagnetic scattering theory*, vol. 93 of *Applied Mathematical Sciences*, Springer-Verlag, Berlin, 1998, second edn., ISBN 3-540-62838-X.
4. V. Rokhlin, *J. Comput. Phys.* **86**, 414–439 (1990), ISSN 0021-9991.
5. V. Rokhlin, *Appl. Comput. Harmon. Anal.* **1**, 82–93 (1993), ISSN 1063-5203.
6. H. Cheng, W. Crutchfield, Z. Gimbutas, L. Greengard, J. Huang, V. Rokhlin, N. Yarvin, and J. Zhao, “Remarks on the implementation of the wideband FMM for the Helmholtz equation in two dimensions,” in *Inverse problems, multi-scale analysis and effective medium theory*, Amer. Math. Soc., Providence, RI, 2006, vol. 408 of *Contemp. Math.*, pp. 99–110.
7. E. Darve, *J. Comput. Phys.* **160**, 195–240 (2000), ISSN 0021-9991.
8. J. M. Song, and W. C. Chew, *Microwave Opt. Tech. Lett.* **10**, 15–19 (1995).
9. B. Engquist, and L. Ying, *SIAM Journal on Scientific Computing* **29**, 1710–1737 (2007).
10. B. Engquist, and L. Ying, Fast directional computation for the high frequency Helmholtz kernel in two dimensions, Tech. rep., University of Texas at Austin (2008).
11. J. B. Keller, *J. Opt. Soc. Amer.* **52**, 116–130 (1962), ISSN 0030-3941.
12. T. Abboud, J.-C. Nédélec, and B. Zhou, *C. R. Acad. Sci. Paris Sér. I Math.* **318**, 165–170 (1994), ISSN 0764-4442.
13. S. N. Chandler-Wilde, and S. Langdon, *SIAM J. Numer. Anal.* **45**, 610–640 (electronic) (2007), ISSN 0036-1429.
14. V. Dominguez, I. G. Graham, and V. P. Smyshlyaev, *Numer. Math.* **106**, 471–510 (2007), ISSN 0029-599X.
15. D. Huybrechs, and S. Vandewalle, *SIAM J. Sci. Comput.* **29**, 2305–2328 (electronic) (2007), ISSN 1064-8275.
16. C. Geuzaine, O. Bruno, and F. Reitich, *Magnetics, IEEE Transactions on* **41**, 1488–1491 (2005), ISSN 0018-9464.
17. L. Greengard, *The rapid evaluation of potential fields in particle systems*, ACM Distinguished Dissertations, MIT Press, Cambridge, MA, 1988, ISBN 0-262-07110-X.
18. L. Greengard, and V. Rokhlin, *J. Comput. Phys.* **73**, 325–348 (1987), ISSN 0021-9991.
19. R. B. Melrose, and M. E. Taylor, *Adv. in Math.* **55**, 242–315 (1985), ISSN 0001-8708.
20. A. Dutt, and V. Rokhlin, *SIAM J. Sci. Comput.* **14**, 1368–1393 (1993), ISSN 1064-8275.
21. O. P. Bruno, and L. A. Kunyansky, *J. Comput. Phys.* **169**, 80–110 (2001), ISSN 0021-9991.
22. W. Burnside, C. Yu, and R. Marhefka, *The Antennas and Propagation Society International Symposium* **11**, 253–256 (1973).
23. U. Jakobus, J. Christ, and F. Landstorfer, *The Eighth IEEE International Conference on Antennas and Propagation* **1**, 111–114 (1993).
24. A. Anand, Y. Boubendir, F. Ecevit, and F. Reitich, Analysis of multiple scattering iterations for high-frequency scattering problems. ii: The three-dimensional scalar case, Tech. rep., Preprint (2006).
25. O. P. Bruno, and C. A. Geuzaine, *J. Comput. Appl. Math.* **204**, 463–476 (2007), ISSN 0377-0427.
26. J.-D. Benamou, F. Collino, and O. Runborg, *J. Comput. Phys.* **199**, 717–741 (2004), ISSN 0021-9991.